

NASA/TM—1998-207424



An Assessment of the Axial and Radial Dilation of a DPIMS Tantalum Cartridge for Space Shuttle Flight Experiments

S.V. Raj and L.J. Ghosn
Lewis Research Center, Cleveland, Ohio

July 1998

The NASA STI Program Office . . . in Profile

Since its founding, NASA has been dedicated to the advancement of aeronautics and space science. The NASA Scientific and Technical Information (STI) Program Office plays a key part in helping NASA maintain this important role.

The NASA STI Program Office is operated by Langley Research Center, the Lead Center for NASA's scientific and technical information. The NASA STI Program Office provides access to the NASA STI Database, the largest collection of aeronautical and space science STI in the world. The Program Office is also NASA's institutional mechanism for disseminating the results of its research and development activities. These results are published by NASA in the NASA STI Report Series, which includes the following report types:

- **TECHNICAL PUBLICATION.** Reports of completed research or a major significant phase of research that present the results of NASA programs and include extensive data or theoretical analysis. Includes compilations of significant scientific and technical data and information deemed to be of continuing reference value. NASA's counterpart of peer-reviewed formal professional papers but has less stringent limitations on manuscript length and extent of graphic presentations.
- **TECHNICAL MEMORANDUM.** Scientific and technical findings that are preliminary or of specialized interest, e.g., quick release reports, working papers, and bibliographies that contain minimal annotation. Does not contain extensive analysis.
- **CONTRACTOR REPORT.** Scientific and technical findings by NASA-sponsored contractors and grantees.

- **CONFERENCE PUBLICATION.** Collected papers from scientific and technical conferences, symposia, seminars, or other meetings sponsored or cosponsored by NASA.
- **SPECIAL PUBLICATION.** Scientific, technical, or historical information from NASA programs, projects, and missions, often concerned with subjects having substantial public interest.
- **TECHNICAL TRANSLATION.** English-language translations of foreign scientific and technical material pertinent to NASA's mission.

Specialized services that complement the STI Program Office's diverse offerings include creating custom thesauri, building customized data bases, organizing and publishing research results . . . even providing videos.

For more information about the NASA STI Program Office, see the following:

- Access the NASA STI Program Home Page at <http://www.sti.nasa.gov>
- E-mail your question via the Internet to help@sti.nasa.gov
- Fax your question to the NASA Access Help Desk at (301) 621-0134
- Telephone the NASA Access Help Desk at (301) 621-0390
- Write to:
NASA Access Help Desk
NASA Center for Aerospace Information
7121 Standard Drive
Hanover, MD 21076

NASA/TM—1998-207424



An Assessment of the Axial and Radial Dilation of a DPIMS Tantalum Cartridge for Space Shuttle Flight Experiments

S.V. Raj and L.J. Ghosn
Lewis Research Center, Cleveland, Ohio

National Aeronautics and
Space Administration

Lewis Research Center

July 1998

Acknowledgments

The authors gratefully acknowledge the comments and suggestions of Randy Bowman, Gil Santoro, and Neil Rowe during the course of this investigation.

Available from

NASA Center for Aerospace Information
7121 Standard Drive
Hanover, MD 21076
Price Code: A03

National Technical Information Service
5287 Port Royal Road
Springfield, VA 22100
Price Code: A03

AN ASSESSMENT OF THE AXIAL AND RADIAL DILATION OF A DPIMS TANTALUM CARTRIDGE FOR SPACE SHUTTLE FLIGHT EXPERIMENTS

S.V. Raj and L.J. Ghosn
National Aeronautics and Space Administration
Lewis Research Center
Cleveland, Ohio 44135

SUMMARY

Ground-based heat treatment tests are planned on an argon gas-filled tantalum cartridge developed as part of a Diffusion Processes in Molten Semiconductors (DPIMS) experiment conducted on NASA's Space Shuttle. The possibility that the cartridge may creep during testing and touch the furnace walls is of real concern in this program. The present paper discusses the results of calculations performed to evaluate this possibility. Deformation mechanism maps were constructed using literature data in order to identify the creep mechanism dominant under the appropriate stresses and temperatures corresponding to the test conditions. These results showed that power-law creep was dominant when the grain size of the material exceeded 55 μm but Coble creep was the important mechanism below this value of grain size. Finite element analysis was used to analyze the heat treatment trials assuming a furnace run away condition (which is a worst case scenario) using the appropriate creep parameters corresponding to grain sizes of 1 and 100 μm . Calculations were also conducted to simulate the effect of an initial 3° tilt of the cartridge assembly (the maximum possible tilt angle). The von Mises stress and strain distributions were calculated assuming that the cartridge was fixed at one end as it was heated from ambient temperature to 1823 K in 1.42 h, maintained at 1823 K for 9.5 h and then further heated to an over temperature condition of 2028 K in 0.3 h. The inelastic axial and radial displacements of the cartridge walls were evaluated by resolving the von Mises strain along the corresponding directions. These calculations reveal that the maximum axial and radial displacements are expected to be about 2.9 and 0.25 mm, respectively, for both fine and coarse-grained materials at 2028 K. It was determined that these displacements occur during heat-up to temperature and creep of the cartridge is likely to be relatively insignificant irrespective of grain size. Furthermore, with a 3° tilt of the cartridge, the deflection is increased by only 0.39 μm which is negligible. Since the gap between the furnace heating elements and the cartridge is about 7.5 mm and less than the maximum radial dilation of 0.25 mm at 2028 K, it is concluded that the cartridge is unlikely to touch the furnace walls during the experiments.

INTRODUCTION

The Diffusion Processes in Molten Semiconductors (DPIMS) experiments were conducted on the first Materials Science Laboratory (MSL-1) payload flight of the Space Shuttle Columbia in 1997. The DPIMS experiment measures the diffusion of germanium at several temperatures using the shear cell technique. Graphite shear cells were enclosed in tantalum cartridges and manually rotated first to align the diffusion columns to begin the diffusion process and later to shear each segment from its neighboring segment, ending the diffusion process (Fig. 1). Prior to flight, these same experiments were conducted in an identical facility on the ground so as to distinguish the role of convection on the diffusion process and to verify the feasibility of the hardware design. In these on-ground tests, each shear cell was rotated against its graphite tab-stop to precisely align the diffusion columns and later counter-rotated to a tab-stop indicating complete shearing of the shear cell segments. In these earlier ground-based tests, the cartridge-shear cell assembly was vertically aligned with the furnace orientations such that the cartridge boss was on top.

During the course of the Space Shuttle experiments, it was observed that the graphite shear cells within the tantalum cartridge failed to operate satisfactorily despite previous success in ground-based trial runs. The Shuttle crew found the torque for rotating the shear cells in space to be very much greater than that experienced during the ground experiments. The Shuttle crew unable to feel the resistance offered by the tab-stops and the shear cells were over rotated. Upon disassembly of the DPIMS cartridge after return to earth, it was discovered that the tabs were still intact and instead, the tantalum rotation tubes and the 304 stainless steel drive shaft had twisted.

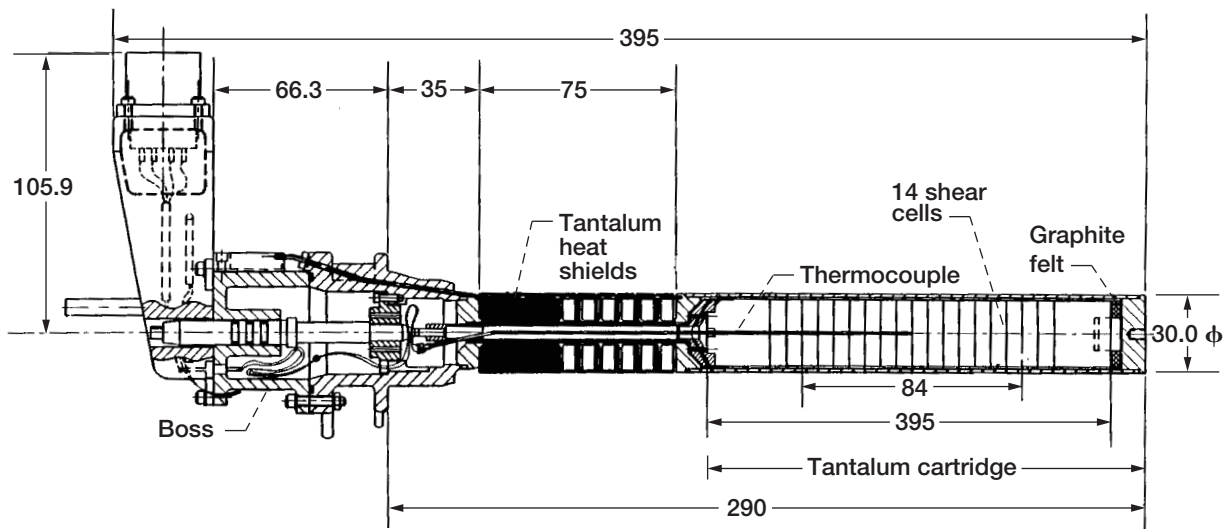


Figure 1.—DPIMS flight cartridge assembly.

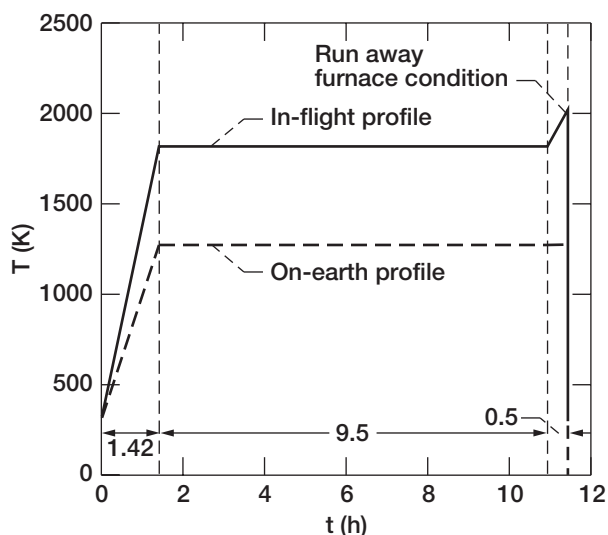


Figure 2.—Temperature-time profiles for the proposed ground-based experiment to be conducted at 1273 K and for a worst-case in-flight scenario with an over temperature condition.

In order to identify the cause of the problem, heat treatment tests are planned on earth, where the cartridge containing the graphite shear cells will be heated from room temperature to 1273 K (1000 °C) and maintained at this temperature for 13 hr and 16 min. The cartridge will be heated in the furnace in an up-side down position so that the gravitational force due to the weight of the cartridge-shear cell assembly will act on the rotation mechanisms. In this configuration, the cartridge boss will be at the bottom. Figure 2 shows the temperature-time profile of the furnace, where T is the absolute temperature and t is time. Two temperature-time profiles are given: (a) the proposed on-earth test profile at 1273 K and (b) the worst case in-space flight scenario assuming a furnace over temperature situation. The cartridges were back-filled with high purity argon gas at 0.10 MPa (1 atm) pressure at room temperature. The design of the cartridge-boss assembly allows free passage of gas between the cartridge and the boss so that the gas is expected to expand from the cartridge to the boss when it is heated to 1273 K (1000 °C) for the ground-based test and to 2028 K (1755 °C) for the in-flight over temperature conditions.

In this study, the worst possible in-flight condition of a run away furnace is considered (Fig. 2). An initial heat-up to 1823K (1550 °C) in 1.42 h is assumed first, followed by a hold for 9.5 h at 1823 K with a final over temperature of 2028 K within half an hour before the final shut down of the furnace (Fig. 2). Calculations by Santoro [1] showed that the gaseous pressures at 1823 and 2028 K were about 0.12 MPa (1.14 atm) and 0.13 MPa (1.27 atm), respectively. As a result of the expansion of the gas during heat-up to 1823 and 2028 K, the cartridge will be under a multiaxial stress state. These gas-pressure induced stresses will act to dilate the cartridge in the axial and radial directions. The axial stress will be countered by the weight of the cartridge, W , acting in the opposite direction. An additional analysis is conducted to determine the effect of the stress due to the weight of the shear cell when the cartridge is tilted by 3° , which is the maximum amount it can tilt due to misalignment. Figure 3 shows the free body diagram of the tilted cartridge with the forces acting on it, where F_r is the radial force, F_{zz} is the axial force and $F_{\theta\theta}$ is the tangential force.

STATEMENT OF THE PROBLEM AND OBJECTIVES

The purpose of this study is to theoretically determine if the cartridge assembly will undergo a large enough deflection of the cartridge walls to cause them to touch the furnace heating elements during the course of the ground-based test. Three factors can cause the walls of the tantalum cartridge to bulge out and/or slump against the furnace heating elements: thermal expansion, creep due to the gas pressure and the weight of the cartridge-shear cell assembly, and tilt forces arising from the noncoaxiality of this assembly and the furnace. Therefore, the objectives of this paper are:

- (a) To identify the dominant creep mechanism using deformation mechanism maps for tantalum.
- (b) To evaluate the magnitudes of the axial and the radial displacements for the in-flight temperature-time profile with a run away furnace condition (Fig. 2). It should be noted that this analysis includes the worst case scenario. The planned ground-based tests will be conducted at a much lower temperature of 1273 K, where the displacements are expected to be much less than the values estimated in this paper.

APPROACH

The present analysis considers the probable effects of the weight of the tantalum cartridge and gas expansion on the axial and radial displacements of the cartridge at the test temperature. An initial study was first conducted to analyze the buckling load required to collapse the tantalum cartridge-shear cell assembly under its own weight assuming that it was co-axial with the furnace. The equation for the Euler buckling load, W , is given by [2]:

$$W = C\pi^2EI / L^2 \quad (1a)$$

where E is Young's modulus of the tantalum cartridge, I is the moment of inertia, L is the length of the cartridge, and C is a constant function of the end constraint. ($C = 1$ for a simply supported tube, and 4 for a tube with clamped-ends). For a tube, $I = \pi(R_{av})^3t_1$ [2], where R_{av} is the average radius of the cartridge, and t_1 is the thickness of the cartridge so that the buckling stress acting on a cross-sectional area, $A = 2\pi R_{av} t_1$ [2], of the cartridge is

$$W / A = C\pi^2E / (L / R_{av})^2 \quad (1b)$$

Substituting the parameters of the tantalum cartridge at a temperature of 2000 K in equation (1a), the load required to buckle the cartridge will be equal to 116,750 Kg, assuming that $E = 1.32 \times 10^5$ MPa at 2000K, $R_{av} = 14.4$ mm, $t_1 = 1.21$ mm, $L = 158.9$ mm, and $C = 1$. This load of 116,750 Kg is much larger than the weight of the tantalum cartridge of about 0.58 Kg. It should be noted that the weight of the tantalum cartridge exerts an axial compressive stress, σ , of less than 0.1 MPa, which is negligible to cause significant creep. The other dominant stress components are due to the gas pressures. The axial, σ_{zz} , hoop, $\sigma_{\theta\theta}$, and radial, σ_r , stresses in a hollow cartridge are given by

$$\sigma_{zz} = p_i R_i / 2t_1 \quad (2a)$$

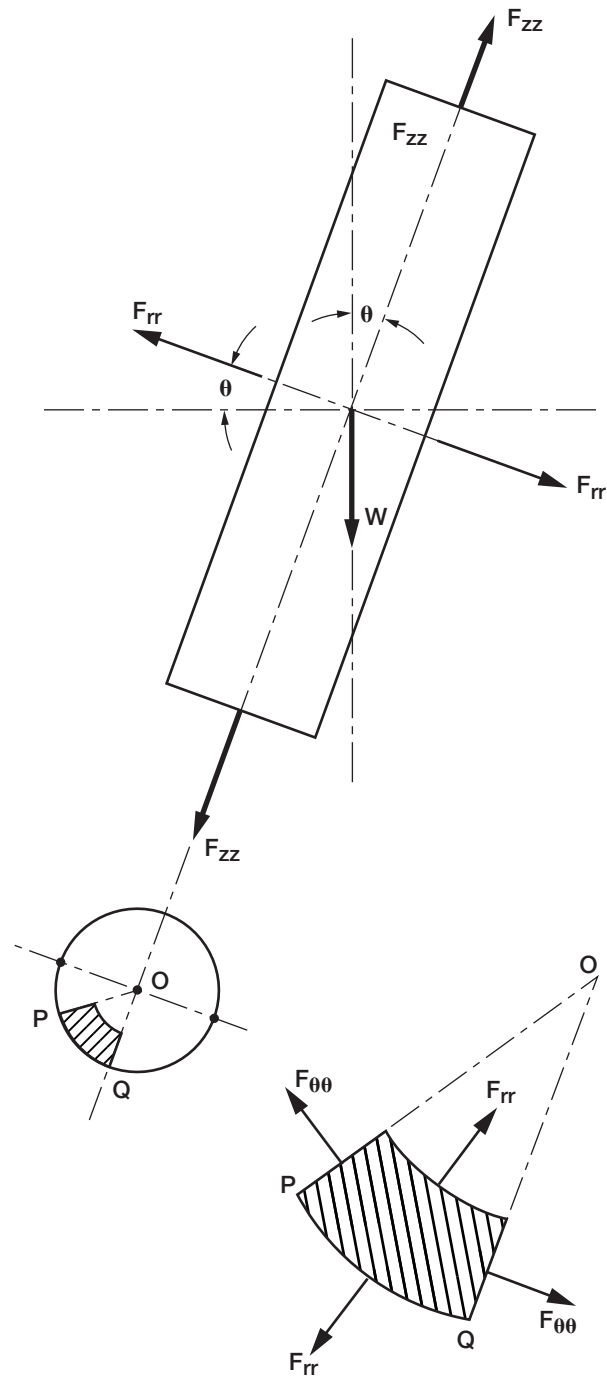


Figure 3.—Free body diagram of the cartridge tilted by θ° . F_{zz} is the axial force, F_{rr} is the radial force, $F_{\theta\theta}$ is the tangential force, and W is the weight of the cartridge-shear cell assembly.

$$\sigma_{\theta\theta} = p_i R_i / t_1 \quad (2b)$$

$$\sigma_{rr} = -p_i (R_i / R)^2 - p_o \left[1 - (R_i / r)^2 \right] \quad (2c)$$

where p_i is the internal gas pressure, p_o is the exterior gas pressure, r is the radius of the cartridge at any arbitrary point, R_i is the internal radius of the cartridge, and R_o is the outer radius of the cartridge. In the present case, $p_o = 0$ at $R = R_o$ and the pressure, p , is $p = p_i$ at $R = R_i$ so that equation (2c) reduces to

$$\sigma_{rr} = (p_i / 2t_1) \left[1 - (2R_i^2 / R^2) (1 + 2t_1 / R_i) \right] \quad (2d)$$

The von Mises stress, σ_{eff} , is then given by

$$\sigma_{\text{eff}} = \left[\frac{1}{2} \left\{ (\sigma_{rr} - \sigma_{\theta\theta})^2 + (\sigma_{\theta\theta} - \sigma_{zz})^2 + (\sigma_{zz} - \sigma_{rr})^2 \right\} \right]^{1/2} \quad (3)$$

In order to evaluate the creep effects on the dimensions of the cartridge, it was necessary to identify the creep mechanism that is likely to be dominant under the test stresses and temperatures. Since some creep mechanisms are dependent on grain size, identification of the dominant creep process was conducted by constructing a deformation mechanism map [3-5]. Three creep mechanisms were considered. The creep rate, $\dot{\epsilon}$, for power-law creep is given by [6]

$$\dot{\epsilon} = A (D_{ol} G b / kT) (\sigma_{\text{eff}} / G)^n \exp(-Q_1 / RT) \quad (4)$$

where A is a dimensionless constant, D_{ol} is the frequency factor for lattice self-diffusion, G is the shear modulus, b is the Burgers vector, k is Boltzmann's constant, n is the stress exponent, Q_1 is the activation energy for lattice self-diffusion and R is the universal gas constant. For Nabarro-Herring creep, the creep rate is given by [4]

$$\dot{\epsilon} = 28 (D_{ol} G b / kT) (b / d)^2 (\sigma_{\text{eff}} / G) \exp(-Q_1 / RT) \quad (5)$$

where d is the grain size. The creep rate for Coble creep is given by [4]

$$\dot{\epsilon} = 66.8 (D_{ogb} G b / kT) (b / d)^3 (\sigma_{\text{eff}} / G) \exp(-Q_{gb} / RT) \quad (6)$$

where D_{ogb} is the frequency factor for grain boundary diffusion and Q_{gb} is the activation energy for grain boundary diffusion.

The deformation maps were constructed by equating the three creep rate equations to obtain the boundaries where the creep rates of the two adjacent mechanisms will be identical [4,5]. The range of stresses and temperatures corresponding to the in-flight conditions that the cartridge is expected to experience are marked on the maps, and the parameters for the corresponding creep mechanism was fed into the finite element analyses (FEM). Steady-state creep was assumed to be dominant and primary creep was ignored in order to simplify the calculations so that the present results are probably an overestimate of the actual dilation of the cartridge.

MATERIAL DATA

The cartridge is made of pure tantalum and the material specification data supplied by the manufacturer are given in Table I. The material from lot number 80557 was used in the actual space flight experiments whereas that from lot 80608 was used in earlier ground-based pre-flight experiments. The physical properties and the creep parameters for this metal have been documented elsewhere [3,7] and they are given in Table II. These data were used for constructing the deformation mechanism maps as well as in the finite element calculations. The grain sizes for the two lots of material were not supplied by the manufacturer. It should be noted that the deformation maps are extremely sensitive to the quality of data used.

TABLE I.—CHEMICAL COMPOSITION IN (WT) PPM AND DIMENSIONS OF THE TANTALUM MATERIALS

Material supplier	Lot number	Description, mm	Chemical composition							
			Mo	Nb	Zr	W	C	H	N	O
Cabot Performance Materials	80557	952.5 × 952.5 × 3.2	<5	30	<5	<25	<10	<5	<10	15
Cabot Performance Materials	80608	482.6 × 482.6 × 3.2	<5	100	<5	25	<10	10	<10	<10

Note: The cartridges were seamless drawn from these materials by B-J Enterprises, Inc. The cartridges were annealed after fabrication.

TABLE II.—DATA USED IN THE FEM CALCULATIONS AND IN THE CONSTRUCTION OF THE DEFORMATION MECHANISM MAPS FOR TANTALUM

Description	Magnitude	Reference
b	2.86×10^{-10} m	[3]
k	1.38×10^{23} J K ⁻¹	[3]
R	8.3×10^{-3} kJ mol ⁻¹ K ⁻¹	[3]
T _m	3271 K	[3]
G	$6.12 \times 10^5 [1 - 0.42(T-300)/3271]$ (MPa)	[3]
D _{0cb}	2.0×10^{-4} m ² s ⁻¹	[3]
Q _{cb}	280 kJ mol ⁻¹	[3]
D _{0l}	1.2×10^{-5} m ² s ⁻¹	[3]
Q _l	413 kJ mol ⁻¹	[3]
n	4.2	[3]
CTE (293-2200 K)	$6.3-10.7 \times 10^{-6}$ K ⁻¹	[7]
v	0.35	[8]

DEFORMATION-MECHANISM MAPS

The deformation maps were constructed by plotting the normalized stress, σ_{eff}/G , against the inverse of the homologous temperature, T_m/T , where T_m is the absolute melting point, for a constant grain size using the procedures described elsewhere [4,5]. Since the grain sizes of the tantalum sheets were unknown, three maps were constructed using grain size values of 10 (Fig. 4(a)), 55 (Fig. 4(b)) and 100 (Fig. 4(c)) μm in order to determine if there is any change in the rate-controlling creep mechanism with decreasing grain size. It was felt that this procedure would allow the finite element analysis to be extended to a larger range of grain sizes, if necessary. The boundaries between two creep mechanisms represent regions of the σ_{eff}/G - T_m/T space, where the creep rates are identical for the two processes. The range of operating conditions corresponding to the test runs are marked on the maps. An examination of Figs. 4(a) to (c) reveals that map boundaries shift to higher values of σ_{eff}/G and T_m/T with decreasing grain size. It is clear from Fig. 4 that for grain sizes less than 55 μm , Coble creep is the dominant creep mechanism, while power-law creep is dominant above this critical value of grain size. However, contributions from Nabarro-Herring creep are relatively small.

Having gained some insight on the dominant creep mechanism for the test conditions, it is sufficient to conduct the FEM analysis assuming that the grain size in the material is above 1 μm . It should be noted that the actual grain size in the material is likely to far exceed 1 μm . As demonstrated in Fig. 4(b), Coble creep becomes important only when $d < 55 \mu\text{m}$ so that the present FEM calculations for a value of $d = 1 \mu\text{m}$ represent the maximum expected axial and radial displacements when Coble creep is dominant. Above $d > 55 \mu\text{m}$, power-law creep is the dominant mechanism and the FEM calculations are independent of grain size.

FINITE ELEMENT ANALYSIS

Finite element analysis was conducted using ABAQUS, which is a commercially available software, where the cartridge was considered to be fixed at the end adjoining the boss and completely free to expand at the end adjoining the graphite felt (Fig. 5). The spatial orientation of the FEM mesh with respect to the cartridge-boss assembly is depicted in Fig. 5. Two models were used in the analysis assuming the worst case temperature-time profile. The first model was a three dimensional analysis to simulate the effect of the tilt of the

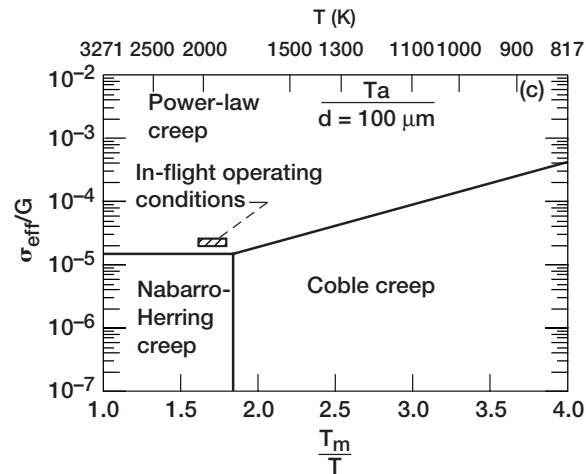
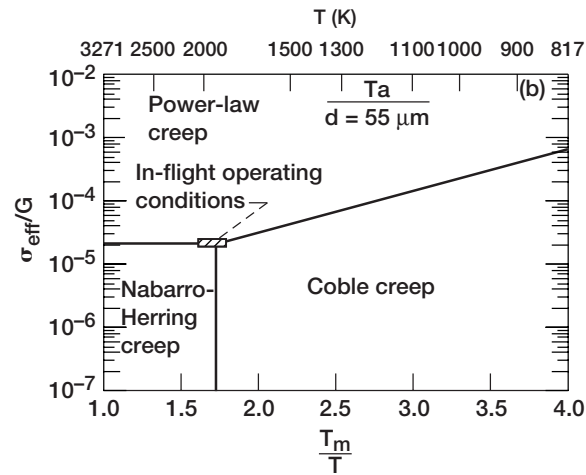
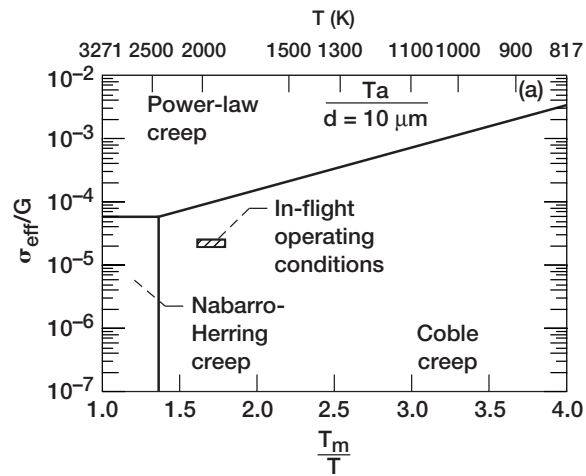


Figure 4.—Deformation mechanism maps plotted as normalized stress, σ/G , against the inverse of the homologous temperature, T_m/T , for grain sizes of (a) $10 \mu\text{m}$, (b) $55 \mu\text{m}$, (c) $100 \mu\text{m}$.

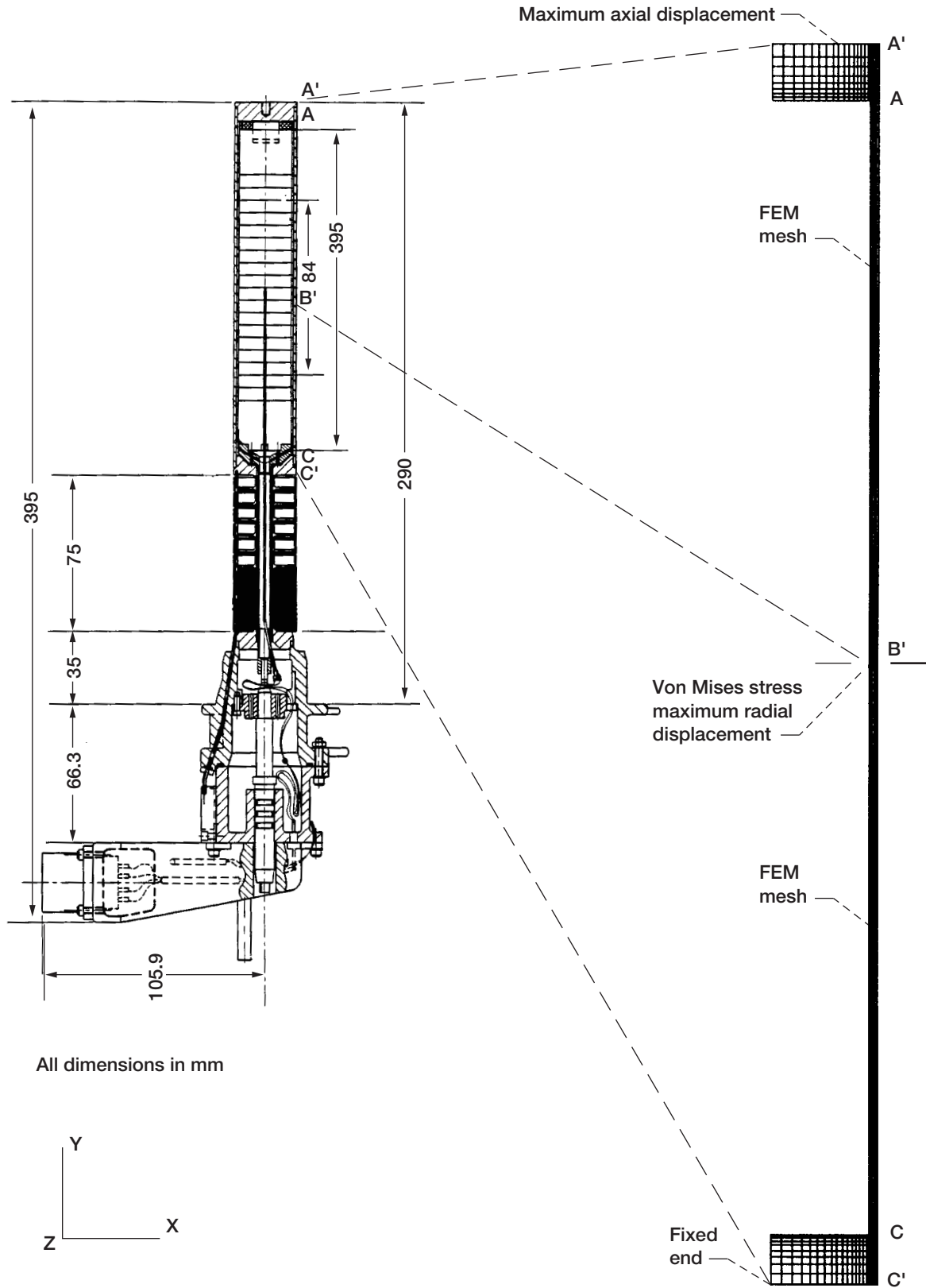


Figure 5.—Schematic showing the orientation of the finite element mesh with respect to the DPIMS flight cartridge assembly.

cartridge by 3° (Fig. 6(a)). This model is deemed relatively crude but a good first approximation. The second model was an axisymmetric analysis, where only a radial cut-off need to be considered which considerably reduces the computational time. Computations were conducted for grain sizes of 1 and $100\ \mu\text{m}$ using the Coble and power-law creep parameters for $d < 55\ \mu\text{m}$ and $d > 55\ \mu\text{m}$, respectively. The materials data for these calculations are given in Table II [3,7,8]. The coefficient of thermal expansion (CTE) for tantalum was obtained from published data [6]. The FEM simulated the worst case scenario of the in-flight experiment, where the cartridge is heated from ambient temperature to 1823 K in 1.42 h, maintained at 1823 K for 9.5 h and then further heated to an over temperature condition of 2028 K in 0.3 h (20 min) (Fig. 2). On reaching 2028 K, it was assumed that the furnace would shut-off and no further FEM calculations were conducted during the subsequent cool down period. The individual stress components determined from Eqs. (2a) to (c) were converted to the von Mises stress given by Eq. (3). The inelastic axial and radial displacements were evaluated by resolving the von Mises strain in the corresponding coordinate directions.

The radial displacements determined by the three dimensional FEM analysis along the normalized axial direction of the tantalum cartridge are shown in Fig. 6(b) when heating it from ambient to the over temperature of 2028 K. The power law creep model was assumed in these calculations. In this analysis, the cartridge assembly was assumed to be tilted 3° from the vertical axis (Fig. 6(a)). The initial shaded area in Fig. 6(b) represents the radial displacement of the cartridge due only to its thermal expansion along the normalized axial length, y/L , where y is an arbitrary axial distance and L is the cartridge length. The hatched region shown in Fig. 6(b) enclosed by the broken line represents the radial displacement of the cartridge due to a maximum possible 3° tilt within the furnace. The maximum deflection due to the non-coaxial tilt of the cartridge is about $0.39\ \mu\text{m}$ at 2028 K. An additional radial displacement due to the gas pressure must also be considered. The total radial displacement along the normalized length of the cartridge due to the combined effects of thermal expansion, cartridge tilt and gas pressure are shown in solid line with a maximum value of about 0.25 mm. This value is well below the clearance of 7.5 mm between the tantalum cartridge and the heating elements even under the worst case scenario considered here. Hence, one can conclude that the cartridge is unlikely to contact the heating elements of the furnace at the intended ground-based test temperature of 1273 K.

Figures 7(a) to (c) show the spatial distribution of the von Mises stress (Fig. 7(a)), the axial (Fig. 7(b)) and radial (Fig. 7(c)) displacements along the length and diameter of the cartridge respectively, at the end of the in-flight heat-up cycle shown in Fig. 2. These calculations assume that $d = 100\ \mu\text{m}$ and power-law creep is the dominant mechanism, and ignore contributions from the cartridge weight which was determined to be negligible. The uncolored grid in Fig. 7 depicts the original position of the cartridge at ambient temperature, while the colored grid represents the final position after heat-up to 2028 K. The von Mises stress varies between 0 and 1.5 MPa, where the maximum stress occurs close to the inside corners of the cartridge (Fig. 7(a)). As shown in Fig. 7(b), the axial displacement, U_{yy} , varies between 0 and 2.9 mm. The radial displacement, U_{xx} , varies from 0 to 0.25 mm (Fig. 7(c)). Figures 8(a) and (b) show the corresponding distributions in the axial and radial strains, respectively. The magnitudes of these strains, which are about 1.7 percent, are relatively constant throughout the cartridge in both the axial and radial directions.

A similar spatial distribution of the von Mises stresses (Fig. 9(a)), axial (Fig. 9(b)) and radial (Fig. 9(c)) displacements are observed when the grain size is $1\ \mu\text{m}$. A decrease in the grain size from 100 to $1\ \mu\text{m}$ results in an increase in the maximum value of σ_{eff} by a factor of about 1.5 due to the dominance of the Coble creep mechanism. However, a comparison of the magnitudes of the axial (Figs. 7(b) and 9(b)) and radial (Figs. 7(c) and 9(c)) displacements for the 1 and $100\ \mu\text{m}$ materials reveals that they are essentially the same. Again, the maximum axial and radial displacements are about 2.9 and 0.25 mm, respectively, thereby suggesting that thermal expansion is more important than creep-induced effects.

Figures 10(a) to (c) show the development of the von Mises stresses at the middle of the cartridge for the fine and coarse-grained materials (Fig. 10(a)) and the axial (Fig. 10(b)) and radial (Fig. 10(c)) displacements of the cartridge walls during the in-flight temperature profile shown in Fig. 2. These values of stress and displacements correspond to the locations shown in Fig. 5. The von Mises stress is slightly higher for the material with a $1\ \mu\text{m}$ grain size than for that with $d = 100\ \mu\text{m}$ (Fig. 10(a)). The maximum axial (Fig. 10(b)) and radial (Fig. 10(c)) displacements are identical for the materials with both grain sizes, thereby confirming that creep-induced effects are negligible. The maximum radial displacement of about 0.25 mm is smaller than the gap between the furnace heating elements and the cartridge, which is about 7.5 mm. Therefore, the cartridge is not expected to touch the furnace heating elements due to radial distortion irrespective of the grain size of the material and any small misalignment.

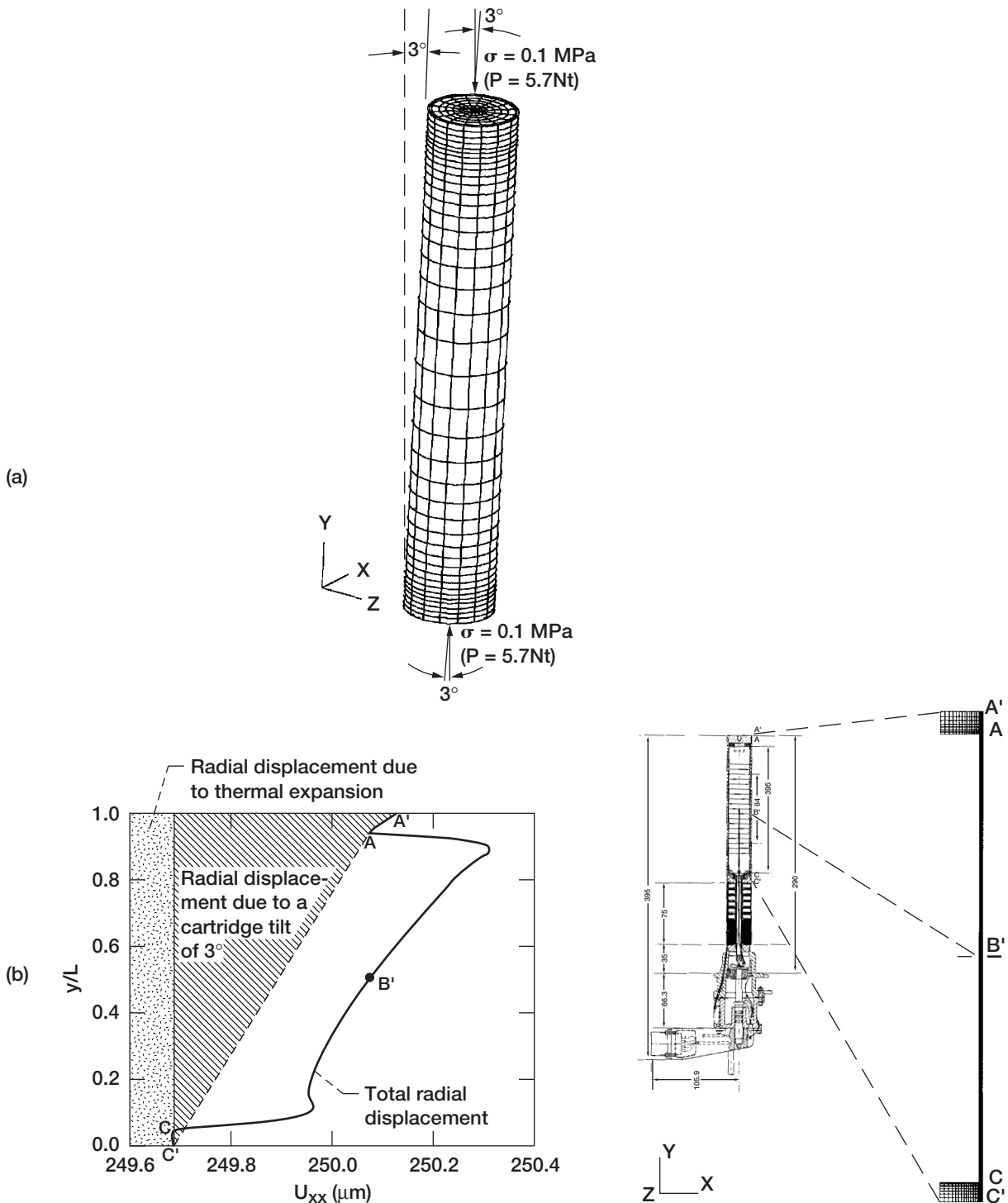


Figure 6.—(a) Schematic view of the three dimensional finite element cylindrical mesh representing a cartridge assembly tilted at 3° inside a furnace. The load, P , acts parallel to the y axis (i. e. parallel to the gravitational force) and the cylinder axis is tilted by 3° from the stress axis. (b) Variation of the radial displacement along the normalized axial length of the DPIMS cartridge. The speckled region represents radial displacement due to only thermal expansion; the hatched region represents the radial displacement due to the 3° tilt of the cartridge; and the solid curve represents the total displacement due to the combined effects of thermal expansion, tilt and gas pressure.

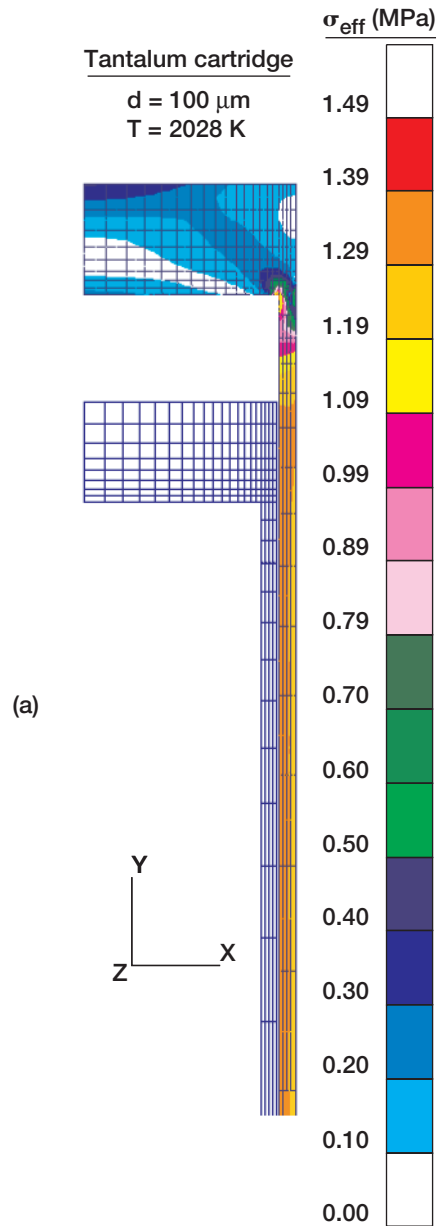


Figure 7.—Spatial distribution of (a) the von Mises stress, and the (b) axial and (c) radial displacements along the length and diameter of the cartridge at the end of the in-flight temperature-time profile shown in Fig. 2. The weight of the cartridge assembly was ignored in these calculations. The grain size of the tantalum cartridge was assumed to be $100 \mu\text{m}$.

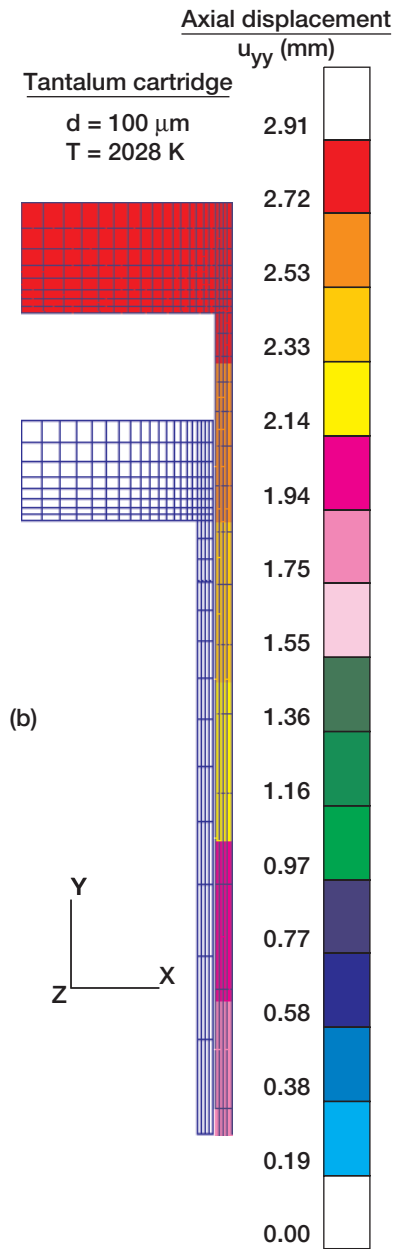


Figure 7.—Continued.

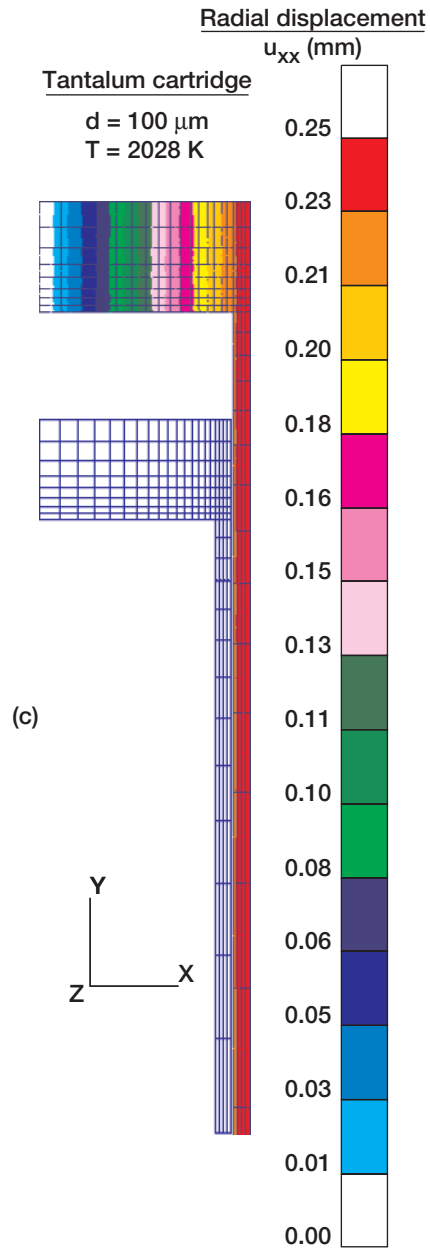


Figure 7.—Concluded.

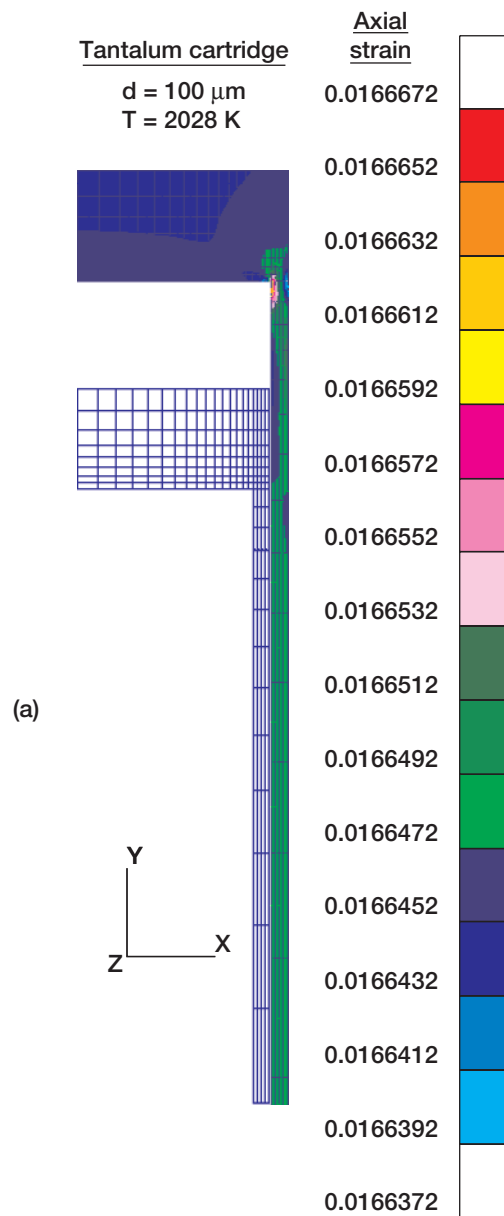


Figure 8.—Distribution of (a) the axial and (b) radial strain along the length and diameter of the cartridge at the end of the in-flight temperature-time profile shown in Fig. 2. The grain size of the tantalum cartridge was assumed to be $100 \mu\text{m}$.

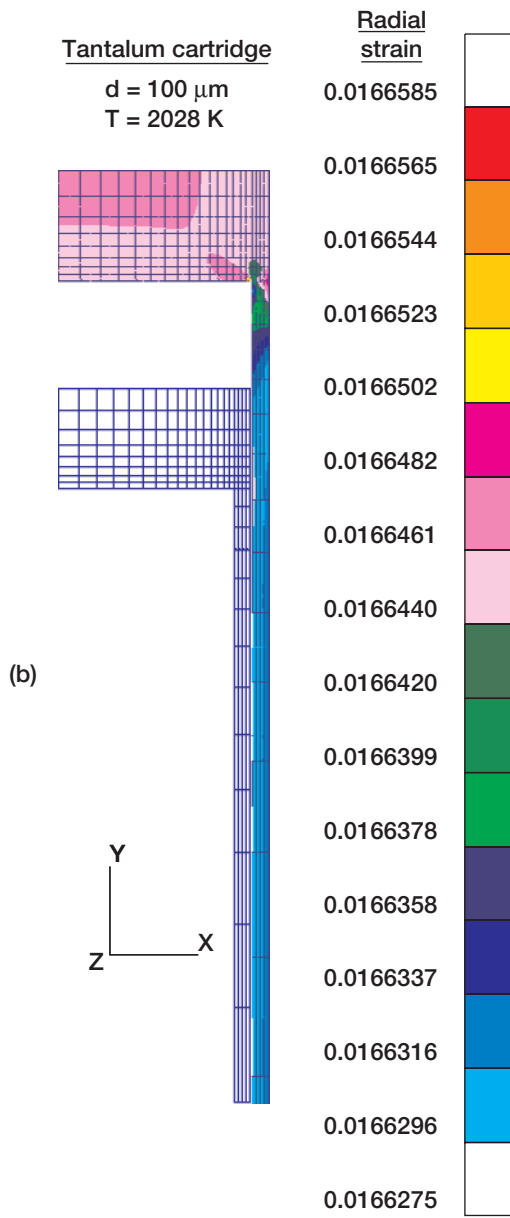


Figure 8.—Concluded.

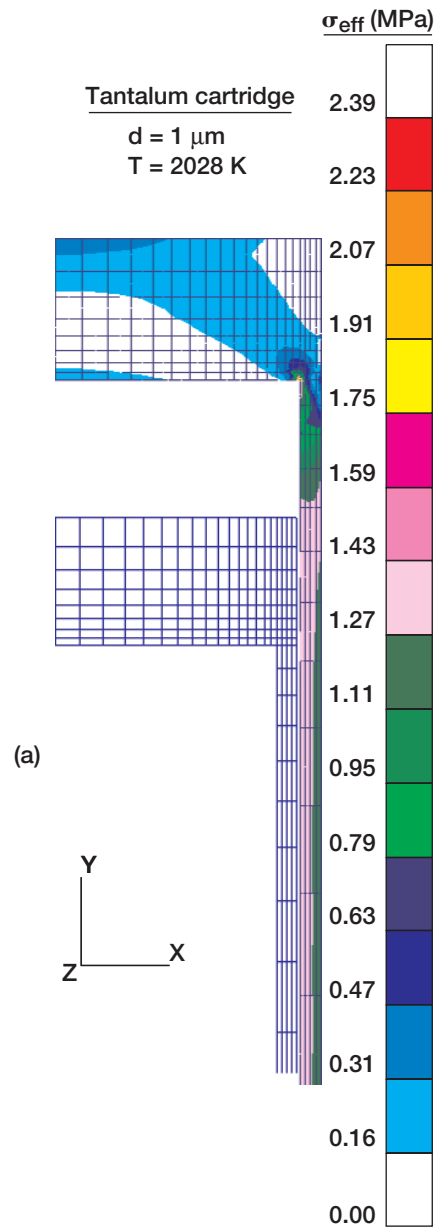


Figure 9.—Spatial distribution of (a) the von Mises stress, and the (b) axial and (c) radial displacements along the length and diameter of the cartridge at the end of the in-flight temperature-time profile shown in Fig. 2. The weight of the cartridge assembly was ignored in these calculations. The grain size of the tantalum cartridge was assumed to be $1 \mu\text{m}$.

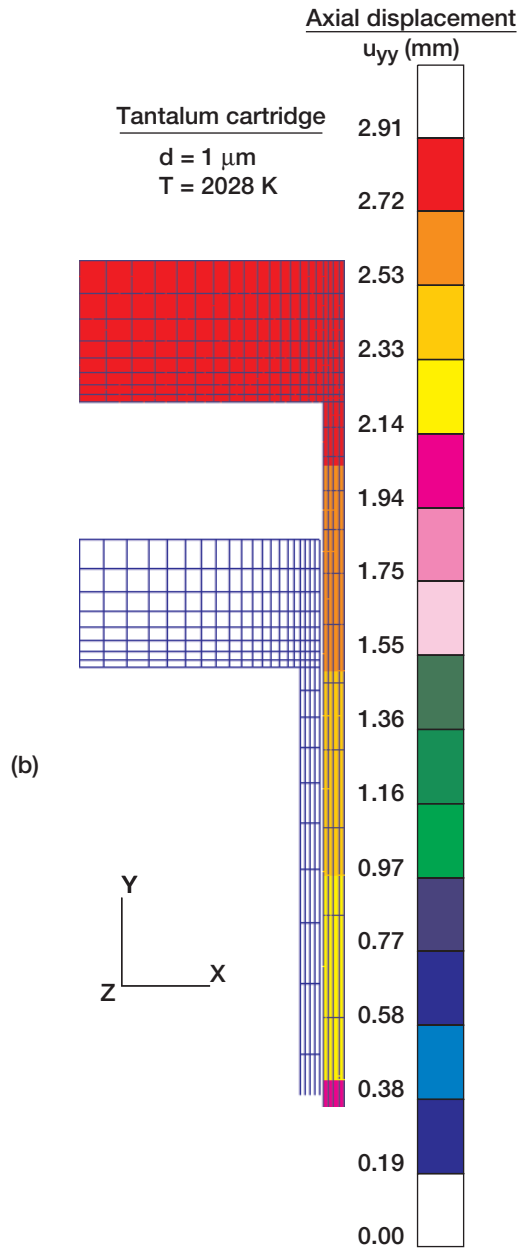


Figure 9.—Continued.

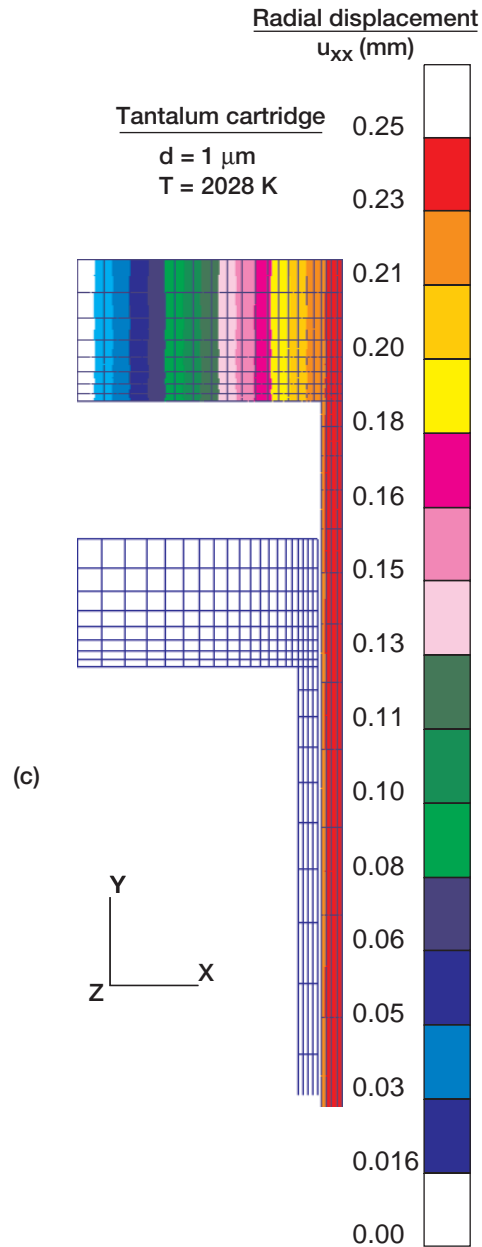


Figure 9.—Concluded.

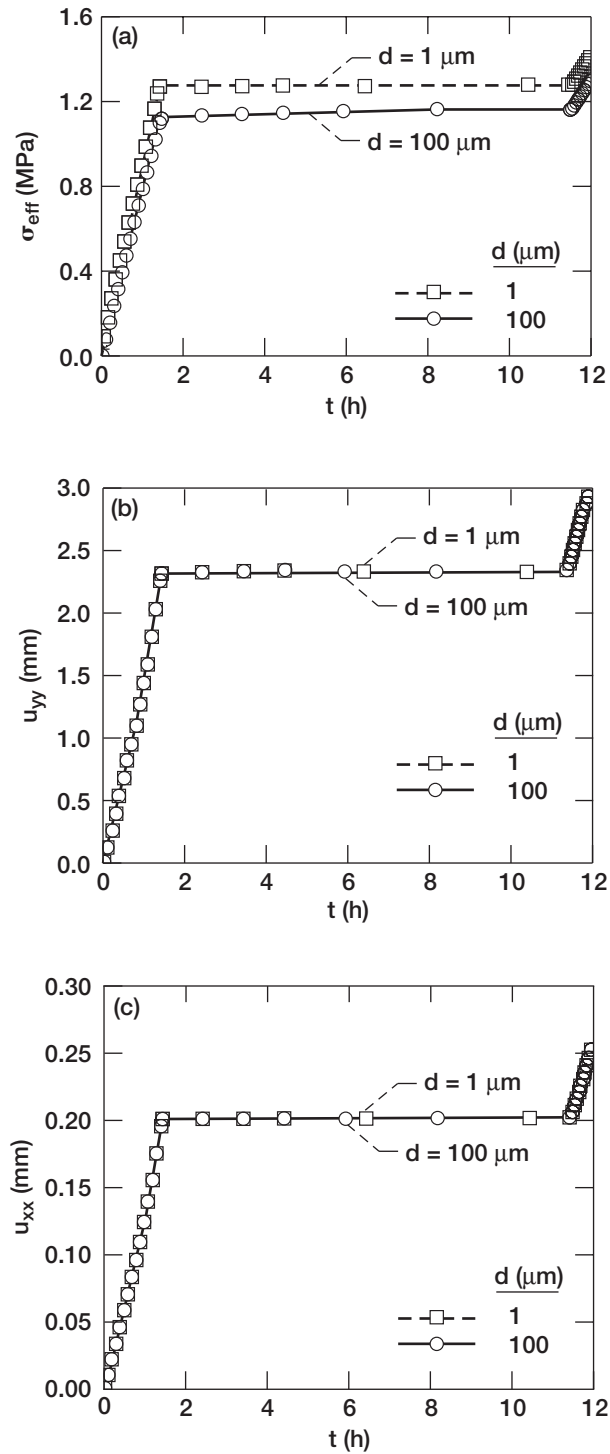


Figure 10.—Development of (a) the von Mises stresses at the middle of the cartridge (B' in Fig. 4), and the (b) axial and (c) radial displacements of the cartridge walls during the in-flight temperature profile depicted in Fig. 2.

SUMMARY AND CONCLUSIONS

Deformation maps were constructed for three grain sizes in order to identify the dominant creep mechanism for the tantalum cartridge under an in-flight run away temperature condition. It is demonstrated that power-law creep will be dominant when the grain size exceeds about 55 μm , while Coble creep will become important below this value of grain size. Using the creep parameters for these two mechanisms, finite element analyses were performed to simulate the run away DPIMS test conditions. These calculations reveal that irrespective of the dominant creep mechanism and grain size of the material, the maximum axial and radial displacements are likely to be less than 3 and 0.25 mm, respectively. A tilt of the cartridge by 3° contributes only a maximum deflection of 0.39 μm at 2028 K. This radial deflection is smaller than the gap between the furnace heating elements and the cartridge, which is about 7.5 mm. Since the calculations made in the present study are for a worst case scenario, the conclusions are valid even for the intended ground-based test temperature of 1273 K. The axial and radial displacements occur primarily due to thermal expansion, and creep-induced distortion of the cartridge is expected to be insignificant for the low values of the estimated gas pressures in the cartridge [1]. In conclusion, the cartridge is not expected to bulge out significantly in the radial direction and touch the furnace heating elements due to creep-induced effects even with a tilt of 3° .

REFERENCES

1. G.J. Santoro, private communication, NASA Lewis Research Center, Cleveland, OH (1997).
2. A.C. Ugural and S.K. Fenster, *Advanced Strength and Applied Elasticity*, Elsevier, New York, (1987).
3. H.J. Frost and M.F. Ashby, *Deformation-Mechanism Maps: The Plasticity and Creep of Metals and Ceramics*, Pergamon Press, Oxford, pp. 32–33 (1982).
4. T.G. Langdon and F.A. Mohamed, *J. Mater. Sci.* 13, 1282 (1978).
5. S.V. Raj and T.G. Langdon, *Mechanical and Corrosion Properties: Single Crystal Properties*, Trans Tech Publications, Aedermannsdorf, Switzerland, pp. 49–47 (1982).
6. J.E. Bird, A.K. Mukherjee and J.E. Dorn, *Quantitative Relation Between Properties and Microstructure* (edited by D. G. Brandon and A. Rosen), Israel Universities Press, Jerusalem, p. 255 (1969).
7. Y.S. Touloukian, R.K. Kirby, R.E. Taylor and P.D. Desai, *Thermal Expansion: Metallic Elements and Alloys*, IFI/Plenum, New York, p. 316, (1975).
8. R.W. Fountain and C.R. McKinsey, *Columbium and Tantalum* (edited by F. T. Sisco and E. Epremian), John Wiley, New York, pp. 198–303, (1963).

REPORT DOCUMENTATION PAGE			Form Approved OMB No. 0704-0188	
Public reporting burden for this collection of information is estimated to average 1 hour per response, including the time for reviewing instructions, searching existing data sources, gathering and maintaining the data needed, and completing and reviewing the collection of information. Send comments regarding this burden estimate or any other aspect of this collection of information, including suggestions for reducing this burden, to Washington Headquarters Services, Directorate for Information Operations and Reports, 1215 Jefferson Davis Highway, Suite 1204, Arlington, VA 22202-4302, and to the Office of Management and Budget, Paperwork Reduction Project (0704-0188), Washington, DC 20503.				
1. AGENCY USE ONLY (Leave blank)	2. REPORT DATE July 1998	3. REPORT TYPE AND DATES COVERED Technical Memorandum		
4. TITLE AND SUBTITLE An Assessment of the Axial and Radial Dilation of a DPIMS Tantalum Cartridge for Space Shuttle Flight Experiments			5. FUNDING NUMBERS WU-963-30-0H-00	
6. AUTHOR(S) S.V. Raj and L.J. Ghosn				
7. PERFORMING ORGANIZATION NAME(S) AND ADDRESS(ES) National Aeronautics and Space Administration Lewis Research Center Cleveland, Ohio 44135-3191			8. PERFORMING ORGANIZATION REPORT NUMBER E-11153	
9. SPONSORING/MONITORING AGENCY NAME(S) AND ADDRESS(ES) National Aeronautics and Space Administration Washington, DC 20546-0001			10. SPONSORING/MONITORING AGENCY REPORT NUMBER NASA TM-1998-207424	
11. SUPPLEMENTARY NOTES Responsible person, S.V. Raj, organization code 5120, (216) 433-8195.				
12a. DISTRIBUTION/AVAILABILITY STATEMENT Unclassified - Unlimited Subject Categories: 18, 26, and 31 This publication is available from the NASA Center for AeroSpace Information, (301) 621-0390.			12b. DISTRIBUTION CODE Distribution: Nonstandard	
13. ABSTRACT (Maximum 200 words) Ground-based heat treatment tests are planned on an argon gas-filled tantalum cartridge developed as part of a Diffusion Processes in Molten Semiconductors (DPIMS) experiment conducted on NASA's Space Shuttle. The possibility that the cartridge may creep during testing and touch the furnace walls is of real concern in this program. The present paper discusses the results of calculations performed to evaluate this possibility. Deformation mechanism maps were constructed using literature data in order to identify the creep mechanism dominant under the appropriate stresses and temperatures corresponding to the test conditions. These results showed that power-law creep was dominant when the grain size of the material exceeded 55 µm but Coble creep was the important mechanism below this value of grain size. Finite element analysis was used to analyze the heat treatment trials assuming a furnace run away condition (which is a worst case scenario) using the appropriate creep parameters corresponding to grain sizes of 1 and 100 µm. Calculations were also conducted to simulate the effect of an initial 3° tilt of the cartridge assembly, the maximum possible tilt angle. The von Mises stress and strain distributions were calculated assuming that the cartridge was fixed at one end as it was heated from ambient temperature to 1823 K in 1.42 h, maintained at 1823 K for 9.5 h and then further heated to an over temperature condition of 2028 K in 0.3 h. The inelastic axial and radial displacements of the cartridge walls were evaluated by resolving the von Mises strain along the corresponding directions. These calculations reveal that the maximum axial and radial displacements are expected to be about 2.9 and 0.25 mm, respectively, for both fine and coarse-grained materials at 2028 K. It was determined that these displacements occur during heat-up to temperature and creep of the cartridge is likely to be relatively insignificant irrespective of grain size. Furthermore, with a 3° tilt of the cartridge, the deflection is increased by only 0.39 µm which is negligible. Since the gap between the furnace heating elements and the cartridge is about 7.5 mm and less than the maximum radial dilation of 0.25 mm at 2028 K, it is concluded that the cartridge is unlikely to touch the furnace walls during the experiments.				
14. SUBJECT TERMS Tantalum; Creep; Finite element analysis; Space shuttle; Diffusion			15. NUMBER OF PAGES 26	
			16. PRICE CODE A03	
17. SECURITY CLASSIFICATION OF REPORT Unclassified	18. SECURITY CLASSIFICATION OF THIS PAGE Unclassified	19. SECURITY CLASSIFICATION OF ABSTRACT Unclassified	20. LIMITATION OF ABSTRACT	